Projecting deep-subwavelength patterns from diffraction-limited masks using metal-dielectric multilayers

Yi Xiong,[1] Zhaowei Liu,[1] and Xiang Zhang[1,2,a)]
[1]*NSF Nanoscale Science and Engineering Center (NSEC), University of California, Berkeley, California 94720, USA*
[2]*Materials Sciences Division, Lawrence Berkeley National Laboratory, 1 Cyclotron Road, Berkeley, California 94720, USA*

(Received 19 August 2008; accepted 28 August 2008; published online 19 September 2008)

We utilize a metal-dielectric multilayer structure to generate deep-subwavelength one-dimensional and two-dimensional periodic patterns with diffraction-limited masks. The working wavelength and the pattern are set by the flexible design of the multilayer structure. This scheme is suitable to be applied to deep-subwavelength photolithography. As an example, we numerically demonstrate pattern periods down to 50 nm under 405 nm light illumination. © *2008 American Institute of Physics*. [DOI: 10.1063/1.2985898]

The rapid progress in the nanoscale science and technology has increased the demand for fabrication of nanoscale patterns. Photolithography is the most widely used microfabrication technique as it is a parallel, cost effective, and high throughput process. However, the conventional photolithography techniques have a resolution barrier due to the diffraction limit of light. To improve the photolithography resolution, one straightforward approach is to reduce the wavelength of the illumination light into deep UV,[1] extreme UV,[2] or even x-ray[3] wavelengths. The main drawbacks of these approaches, however, are the drastically increased instrument complexity and the corresponding cost. Several other techniques are also available to achieve nanoscale feature sizes: electron-beam lithography,[4] focused ion-beam lithography,[5] dip-pen lithography,[6,7] and imprint lithography,[8,9] just to name a few. Although these techniques have been widely used, each of them has to face its own disadvantages.

Recently, plasmonic nanolithography[10–17] was demonstrated to improve the photolithography resolution by utilizing surface plasmons. The wavelength of surface plasmons is smaller than that of light in free space at the same frequency.[18] Hence, photolithography assisted with surface plasmons can generate patterns with subwavelength feature sizes. Furthermore, plasmonic nanolithography is completely compatible with conventional photolithography as they both share the same optical frequency and process flow.

Near field contact lithography is another promising subdiffraction-limited photolithography method, which forms patterns with subdiffraction-limited resolution in the near field of the mask.[19–21] However, the patterns formed by the near field contact lithography are identical to the masks. Therefore, subdiffraction-limited masks are always required to form subdiffraction-limited patterns.

In this paper, we propose a deep-subwavelength photolithography method which uses a designed metal-dielectric multilayer to generate the subwavelength features from a traditional one-dimensional (1D) or two-dimensional (2D) diffraction-limited mask (see Fig. 1). By designing the optical transfer function of the multilayer structure, we can adjust the period ratio between the diffraction-limited mask and the deep-subwavelength lithographic pattern.

For simplicity, we consider a 1D periodic mask with period Λ (Λ is larger than the diffraction limit) to illustrate the principle, which can be extended to the case of 2D periodic masks easily. Let us define x as the grating direction of the 1D periodic mask and z as the direction perpendicular to the grating plane [see Fig. 2(b)]. The waves emerging from the mask are the sum of a series of diffracted plane waves, $\Sigma_{i=-\infty}^{\infty} T^{(i)} \exp[j(k_x^{(i)}x + k_z^{(i)}z)]$, where $k_x^{(i)} = i2\pi/\Lambda$, $[k_z^{(i)}]^2 = (n2\pi/\lambda)^2 - [k_x^{(i)}]^2$, where i is an integer diffraction order, $T^{(i)}$ is the amplitude of ith order plane wave, λ is the wavelength of the incident light in free space, and n is the refractive index of the medium on the transmission side of the grating. Depending on whether $[k_z^{(i)}]^2$ is larger or smaller than zero, the diffracted plane wave is propagating or evanescent, respectively. The evanescent waves carry subdiffraction-limited information of the mask but decay exponentially with the distance away from the mask. Therefore in conventional projection photolithography, the evanescent waves play no role, and the resolution is diffraction-limited. By including the evanescent waves, near field contact lithography forms subdiffraction-limited patterns in the near field of the mask but requires subdiffraction-limited masks.

In our approach of photolithography, we generate subdiffraction-limited patterns from a diffraction-limited mask, using a special slab of material that only allows waves

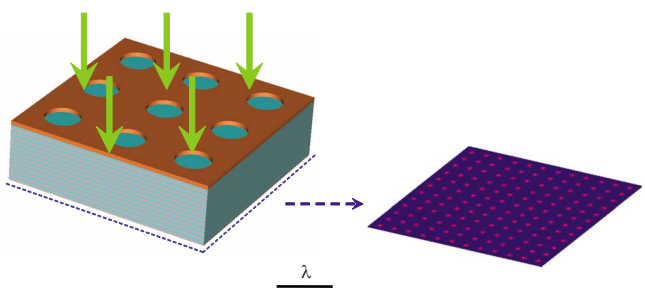

FIG. 1. (Color online) Schematic of deep-subwavelength photolithography using metal-dielectric multilayer.

a)Author to whom correspondence should be addressed. Electronic mail: xiang@berkeley.edu.

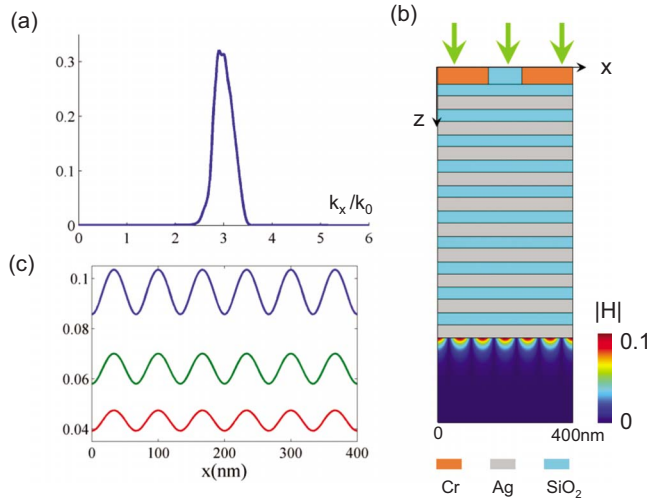

FIG. 2. (Color online) (a) The transmission vs the tangential wavevector for a 10 pairs of 40 nm Ag and 35 nm SiO_2 multilayer. The polarization is TM polarization. Working wavelength is 405 nm. (b) Configuration for photolithography and the simulated $|H|$ field after the multilayer. Only one period (400 nm) of the grating mask is shown. (c) The $|E|$ field in the photoresist at the multilayer-photoresist interface (blue), 10 nm (green), and 20 nm (red) away from the interface.

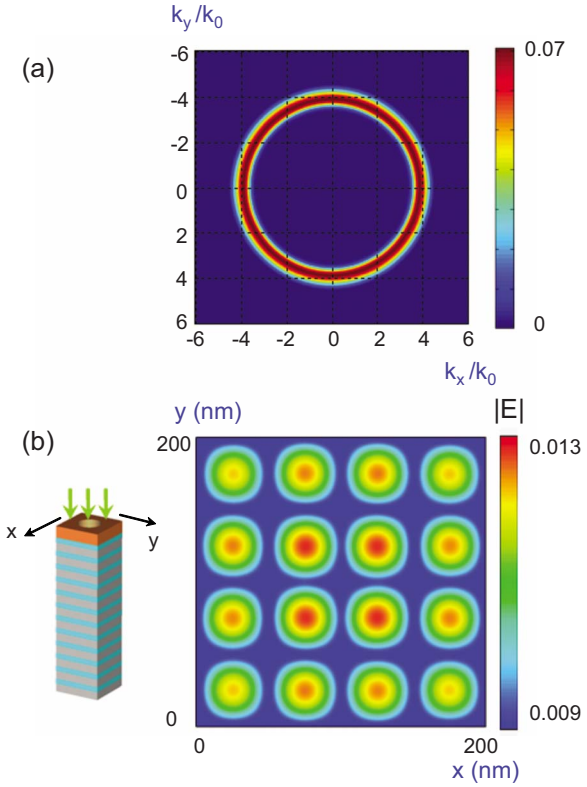

FIG. 3. (Color online) (a) The transmission vs tangential wavevector k_x and k_y (2D transfer function) for a 12 pairs of 35 nm Ag and 21 nm SiO_2 multilayer at a wavelength of 405 nm. (b) The simulated $|E|$ field at the plane 3 nm after the Ag and SiO_2 multilayer. The left inset is the configuration for photolithography. Only one period (200 nm) is shown.

with tangential wave vector larger than nk_0 ($k_0=2\pi/\lambda$) to pass through. Furthermore, the width of the spatial frequency pass band is narrow enough to allow one diffraction order ($\pm m$th order) from the 1D mask only. When we place this slab material immediately after a diffraction-limited mask, a subdiffraction-limited pattern with period $\Lambda/2m$ is formed on the other side of the slab material as a result of the superposition of the $\pm m$th order diffraction waves.

The abovementioned special slab material can be realized by a metamaterial, an artificial fabricated structure that has received significant attention recently because of its properties that are not observed in nature.[22–24] A metal-dielectric multilayer structure, one of the simplest metamaterials, has been proposed for various applications.[25–29] As an example, we shall show a designed slab of multilayer metamaterial can realize the deep-subwavelength photolithography. A metal-dielectric multilayer has those special properties because of the split surface plasmon modes on the metal-dielectric multilayer. Surface plasmon modes split on a metal thin film due to the interaction of modes on two metal surfaces.[30] As the number of the metal thin films increases, the number of the split surface plasmon modes increases accordingly.[31] With proper design, the split surface plasmon modes can be highly compacted, and form a band. Subsequently, the transmission (through the multilayer) of a range of tangential wavevector band corresponding to the surface plasmon mode band is large and the transmission of the rest tangential wavevector band is negligible. Therefore, the designed multilayer can act as an extraordinary spatial filter, i.e., only allows a band of waves with tangential wavevector larger than nk_0 to go through it. The location and the bandwidth of the pass band can be tuned by changing the thicknesses of the metal and dielectric layers.[32]

We firstly show one example where a metal-dielectric multilayer can generate a deep-subwavelength 1D pattern from a diffraction-limited mask. Figure 2(a) shows the transmission versus the tangential wavevector (transfer function) for a 10 pairs of 40 nm Ag and 35 nm SiO_2 multilayer for TM polarization at a wavelength of 405 nm. The permittivity of Ag is $-4.67+0.22i$.[33] The permittivity of SiO_2 is 2.16.[34] The permittivity of the photoresist after the multilayer is 2.89 (negative photoresist NFR 105 G from JSR Micro). From the transfer function of the multilayer, only a band of waves with tangential wavevector around $3k_0$ can pass through this structure. If a grating mask with 400 nm period is added in front of the multilayer structure and illuminated by a light at 405 nm, only the ± 3 order diffraction waves from the mask can go through the multilayers and form a pattern with period six times smaller compared with the mask. This spatial frequency sextupling effect is evidently shown by the simulated $|H|$ field distribution (COMSOL MULTIPHYSICS 3.4) after the multilayer in Fig. 2(b). The thickness of the Cr mask is 50 nm, and the opening width is 100 nm. For photolithography purpose, the $|E|$ field distribution is also shown in Fig. 2(c) at planes 0, 10, and 20 nm after the Ag and SiO_2 multilayer. The intensity contrast is $(|E|^2_{max}-|E|^2_{min})/(|E|^2_{max}+|E|^2_{min})\approx 0.2$, which satisfies the minimum contrast required for common negative photoresists.[35]

The above method can be easily extended to 2D patterns generation, as illustrated by the following example: Additionally, we redesign the Ag–SiO_2 multilayer to show that different period ratio between the mask and the lithographic pattern is achievable by adjusting the configuration of the multilayer. Figure 3(a) is the 2D transfer function (the transmission versus tangential wavevector k_x and k_y) for a 12 pairs of 35 nm Ag and 21 nm SiO_2 multilayer at a wavelength of 405 nm. Each set of k_x and k_y can define an incident plane. The 2D transfer function is calculated in the way

that the H field is always perpendicular to the incident plane corresponding each set of k_x and k_y (see Ref. 32 for more about the 2D transfer function). In this exampled case, we design the multilayer to allow the transmission of the waves with tangential wavevector $k=\sqrt{k_x^2+k_y^2}$ around $4k_0$. The mask is a 2D grating with square lattice on a 50 nm thickness Cr slab. The period is 200 nm, and the diameter of the circular opening is 100 nm [see the left inset of Fig. 3(b), one unit cell is shown]. Only the ± 2 order diffracted waves from the mask have tangential wavevector $2\times 405/200k_0 \approx 4k_0$ thus can propagate through the multilayer. As a result, a pattern with period $200/(2\times 2)=50$ nm is formed after the multilayer. Figure 3(b) is the $|E|$ field at the plane 3 nm after the multilayer calculated by CST Microwave Studio 2008. In the simulation, the incident light has circular polarization. The multilayer selects the TM polarized direction for each set of k_x and k_y, and allows the transmission of the waves with tangential wavevector $k=\sqrt{k_x^2+k_y^2}$ around $4k_0$. The intensity contrast of E field is about 0.3, larger than the minimum intensity contrast required by common negative photoresist.[35]

As a summary, we numerically demonstrated a photolithography scheme that can fabricate deep-subwavelength nanometer scale 1D and 2D periodic patterns from diffraction-limited masks. We can determine the period ratio between the mask and the photolithography pattern by designing the multilayer structure. At wavelength of 405 nm, we obtained a 1D periodic pattern with 67 nm period from a 1D mask with 400 nm period. We also demonstrated a 2D periodic pattern with 50 nm period from a 2D mask with 200 nm period. Our technique provides a cost effective mass production method to fabricate deep-subwavelength patterns. The mask used in our method, which is diffraction limited, can be fabricated by conventional photolithography or laser interference lithography.

The authors thank Dr. Guy Bartal and Dr. Stephane Durant for valuable discussions. This work was supported by the National Science Foundation (NSF) Nanoscale Science and Engineering Center (Grant No. DMI-0327077) and the Air Force Office of Scientific Research (AFOSR), the Multidisciplinary University Research Initiative (MURI) (Grant No. FA9550-04-1-0434).

[1] A. K. Bates, M. Rothschild, T. M. Bloomstein, T. H. Fedynyshyn, R. R. Kunz, V. Liberman, and M. Switkes, IBM J. Res. Dev. **45**, 605 (2001).
[2] C. W. Gwyn, R. Stulen, D. Sweeney, and D. Attwood, J. Vac. Sci. Technol. B **16**, 3142 (1998).
[3] J. P. Silverman, J. Vac. Sci. Technol. B **16**, 3137 (1998).
[4] C. Vieu, F. Carcenac, A. Pepin, Y. Chen, M. Mejias, A. Lebib, L. Manin-Ferlazzo, L. Couraud, and H. Launois, Appl. Surf. Sci. **164**, 111 (2000).
[5] J. Melngailis, A. A. Mondelli, I. L. Berry, and R. Mohondro, J. Vac. Sci. Technol. B **16**, 927 (1998).
[6] R. D. Piner, J. Zhu, F. Xu, S. Hong, and C. A. Mirkin, Science **283**, 661 (1999).
[7] D. S. Ginger, H. Zhang, and C. A. Mirkin, Angew. Chem. **43**, 30 (2004).
[8] S. Y. Chou, P. R. Krauss, and P. J. Renstrom, Science **272**, 85 (1996).
[9] H. Schift, J. Vac. Sci. Technol. B **26**, 458 (2008).
[10] R. J. Blaikie and S. J. McNab, Appl. Opt. **40**, 1692 (2001).
[11] W. Srituravanich, N. Fang, C. Sun, Q. Luo, and X. Zhang, Nano Lett. **4**, 1085 (2004).
[12] X. G. Luo and T. Ishihara, Opt. Express **142**, 3055 (2004).
[13] Z. W. Liu, Q. H. Wei, and X. Zhang, Nano Lett. **5**, 957 (2005).
[14] W. Srituravanich, S. Durant, H. Lee, C. Sun, and X. Zhang, J. Vac. Sci. Technol. B **23**, 2636 (2005).
[15] D. B. Shao and S. C. Chen, Appl. Phys. Lett. **86**, 253107 (2005).
[16] A. Sundaramurthy, P. J. Schuck, N. R. Conley, D. P. Fromm, G. S. Kino, and W. E. Moerner, Nano Lett. **6**, 355 (2006).
[17] L. Wang, S. M. Uppuluri, E. X. Jin, and X. F. Xu, Nano Lett. **6**, 361 (2006).
[18] W. L. Barnes, A. Dereux, and T. W. Ebbesen, Nature (London) **424**, 824 (2003).
[19] M. M. Alkaisi, R. J. Blaikie, S. J. McNab, R. Cheung, and D. R. S. Cumming, Appl. Phys. Lett. **75**, 3560 (1999).
[20] J. G. Goodberlet and H. Kavak, Appl. Phys. Lett. **81**, 1315 (2002).
[21] D. O. S. Melville and R. J. Blaikie, J. Vac. Sci. Technol. B **22**, 3470 (2004).
[22] R. A. Shelby, D. R. Smith, and S. Schultz, Science **292**, 77 (2001).
[23] D. Schurig, J. J. Mock, B. J. Justice, S. A. Cummer, J. B. Pendry, A. F. Starr, and D. R. Smith, Science **314**, 977 (2006).
[24] Z. W. Liu, H. Lee, Y. Xiong, C. Sun, and X. Zhang, Science **315**, 1686 (2007).
[25] N. N. Lepeshkin, A. Schweinsberg, G. Piredda, R. S. Bennink, and R. W. Boyd, Phys. Rev. Lett. **93**, 123902 (2004).
[26] P. A. Belov and Y. Hao, Phys. Rev. B **73**, 113110 (2006).
[27] B. Wood, J. B. Pendry, and D. P. Tsai, Phys. Rev. B **74**, 115116 (2006).
[28] H. C. Shin and S. H. Fan, Appl. Phys. Lett. **89**, 151102 (2006).
[29] M. Scalora, M. J. Bloemer, A. S. Pethel, J. P. Dowling, C. M. Bowden, and A. S. Manka, J. Appl. Phys. **83**, 2377 (1998).
[30] E. N. Economou, Phys. Rev. **182**, 539 (1969).
[31] I. Avrutsky, I. Salakhutdinov, J. Elser, and V. Podolskiy, Phys. Rev. B **75**, 241402 (2007).
[32] Y. Xiong, Z. W. Liu, C. Sun, and X. Zhang, Nano Lett. **7**, 3360 (2007).
[33] P. B. Johnson and R. W. Christy, Phys. Rev. B **6**, 4370 (1972).
[34] E. D. Palik, *Handbook of Optical Constants of Solids* (San Diego, Academic, 1998).
[35] M. J. Madou, *Fundamentals of Microfabrication* (CRC, Boca Raton, 2002).